*J. Phycol.* **48,** 595–606 (2012)

DOI: 10.1111/j.1529-8817.2012.01166.x

# NITROGEN FIXATION, HYDROGEN CYCLING, AND ELECTRON TRANSPORT KINETICS IN *TRICHODESMIUM ERYTHRAEUM* (CYANOBACTERIA) STRAIN IMS101[1]

*Samuel T. Wilson*[2]

Center for Microbial Oceanography: Research and Education, University of Hawaii, 1950 East-West Road, Honolulu, Hawaii 96822, USA

*Zbigniew S. Kolber, Sasha Tozzi, Jonathan P. Zehr*

Ocean Sciences, University of California, Santa Cruz, California 95064, USA

*and David M. Karl*

Center for Microbial Oceanography: Research and Education, University of Hawaii, 1950 East-West Road, Honolulu, Hawaii 96822, USA

**This study describes the relationships between dinitrogen ($N_2$) fixation, dihydrogen ($H_2$) production, and electron transport associated with photosynthesis and respiration in the marine cyanobacterium *Trichodesmium erythraeum* Ehrenb. strain IMS101. The ratio of $H_2$ produced:$N_2$ fixed ($H_2$:$N_2$) was controlled by the light intensity and by the light spectral composition and was affected by the growth irradiance level. For *Trichodesmium* cells grown at 50 μmol photons · $m^{-2}$ · $s^{-1}$, the rate of $N_2$ fixation, as measured by acetylene reduction, saturated at light intensities of 200 μmol photons · $m^{-2}$ · $s^{-1}$. In contrast, net $H_2$ production continued to increase with light levels up to 1,000 μmol photons · $m^{-2}$ · $s^{-1}$. The $H_2$:$N_2$ ratios increased monotonically with irradiance, and the variable fluorescence measured using a fast repetition rate fluorometer (FRRF) revealed that this increase was accompanied by a progressive reduction of the plastoquinone (PQ) pool. Additions of 2,5-dibromo-3-methyl-6-isopropyl-p-benzoquinone (DBMIB), an inhibitor of electron transport from PQ pool to PSI, diminished both $N_2$ fixation and net $H_2$ production, while the $H_2$:$N_2$ ratio increased with increasing level of PQ pool reduction. In the presence of 3-(3,4-dichlorophenyl)-1,1-dimethylurea (DCMU), nitrogenase activity declined but could be prolonged by increasing the light intensity and by removing the oxygen supply. These results on the coupling of $N_2$ fixation and $H_2$ cycling in *Trichodesmium* indicate how light intensity and light spectral quality of the open ocean can influence the $H_2$:$N_2$ ratio and modulate net $H_2$ production.**

*Key index words:* **bioenergetics; hydrogen; nitrogen fixation; photosynthesis; *Trichodesmium***

*Abbreviations:* **σPSII, functional absorption cross-section; ϕPSII, the efficiency of charge separation; $C_2H_2$, acetylene; $C_2H_4$, ethylene; DBMIB, 2,5-dibromo-3-methyl-6-isopropyl-p-benzoquinone; DCMU, 3-(3, 4-dichlorophenyl)-1,1-dimethylurea; FQR, ferredoxin:quinone oxireductase; FRRF, fast repetition rate fluorometer; G3P, glyceraldehyde-3-phosphate; Ndh, NAD(P) dehydrogenase; OPP, oxidative pentose phosphate cycle; PC, plastocyanine; PETR, photosynthetic electron transport rate; PQ, plastoquinone; RC, reaction centers**

*Trichodesmium* is a filamentous, nonheterocystous cyanobacterium inhabiting the surface waters of tropical and subtropical marine environments (Capone et al. 1997). In the oligotrophic ocean, the fixation of $N_2$ by *Trichodesmium* and other diazotrophs is an important source of new nitrogen (N) that fuels primary production and export in the surface seawater (Dugdale and Goering 1967, Karl 2007). Among the diazotrophs, *Trichodesmium* has the distinctive metabolic capability of fixing $N_2$ during daylight while simultaneously fixing carbon dioxide ($CO_2$) and releasing oxygen ($O_2$). $O_2$ is a potent inhibitor of the enzyme nitrogenase, which catalyzes $N_2$ fixation (Postgate 1982). However, by synchronizing $N_2$ fixation with photosynthesis, *Trichodesmium* is able to supply nitrogenase with solar-derived energy (Berman-Frank et al. 2007).

In addition to the marine N cycle, *Trichodesmium* and other $N_2$-fixing cyanobacteria also contribute to the marine hydrogen ($H_2$) cycle. $H_2$ is formed during $N_2$ fixation when a $N_2$ molecule binds to the molybdenum-iron protein of the nitrogenase enzyme complex, prior to the reduction of $N_2$ to ammonia ($NH_3$) (Lowe and Thorneley 1984). The

[1]Received 12 May 2011. Accepted 18 October 2011.
[2]Author for correspondence: e-mail stwilson@hawaii.edu.

most energetically favorable stoichiometry predicts that at least one mole of $H_2$ is produced for every mole of $N_2$ reduced:

$$N_2 + (6 + 2n)H^+ + (6 + 2n)e^- + 2(6 + 2n)ATP \rightarrow 2NH_3 + (n)H_2 + 2(6 + 2n)(ADP + 16Pi) \quad (1)$$

where $n \geq 1.0$, hydrogen ion is $H^+$, electron is $e^-$, adenosine triphosphate is ATP, adenosine diphosphate is ADP, and inorganic phosphate is Pi (Simpson and Burris 1984). The evolution of $H_2$ during $N_2$ fixation by marine diazotrophs is considered to be responsible for the supersaturation of dissolved $H_2$ in the surface waters of subtropical and tropical oceans (Scranton 1983, Conrad 1988, Moore et al. 2009). Dissolved $H_2$ concentrations typically range from 1 to 2 nmol $\cdot$ $L^{-1}$, which is ~300%–900% supersaturated relative to atmospheric equilibrium (Seiler and Schmidt 1974).

Although it is unclear what controls the net $H_2$ production during $N_2$ fixation, it appears that diazotrophs counteract the loss of this potential energy by reassimilating a variable portion of $H_2$ via uptake hydrogenase (Tamagnini et al. 2007). The electrons generated from $H_2$ oxidation are transferred from uptake hydrogenase to PQ supplementing the photosynthetic electron flow mediated by PSI. These electrons may (i) contribute to energy production through the mechanisms of cyclic electron flow around PSI, (ii) replenish reducing power in the form of NADH, (iii) recycle electrons in the $N_2$-fixation pathway, (iv) undergo a ''Knallgas'' reaction generating ATP with the simultaneous consumption of $O_2$ (Eisbrenner and Bothe 1979), or (v) complete the respiratory pathway toward the terminal cytochrome oxidase. The recycling of $H_2$ evolved during $N_2$ fixation explains why the equimolar ratio of $H_2$ produced to $N_2$ fixed ($H_2$:$N_2$) predicted in equation 1 is not observed during *in vivo* analysis of diazotrophs cultures (Bothe et al. 1980, Wilson et al. 2010a).

Dihydrogen production and $N_2$ fixation associated with *Trichodesmium* spp. has been measured in field-collected colonies (Saino and Hattori 1982, Scranton 1983, Scranton et al. 1987) and in laboratory-maintained cultures of *T. erythraeum* IMS101 (Punshon and Moore 2008, Wilson et al. 2010a). The reported $H_2$:$N_2$ production ratios for *Trichodesmium* reach 0.3, indicating that 30% of the $H_2$ evolved during the $N_2$-fixation process is not re-assimilated. Such a high fraction of unassimilated $H_2$ is suggestive of an inefficient $N_2$-fixation process with respect to energy utilization (Schubert and Evans 1976). High $H_2$ fluxes have also been identified in other cyanobacteria (e.g., *Nostoc*, *Anabaena*; Schütz et al. 2004, Allahverdiyeva et al. 2010) and more recently in the unicellular cyanobacterium *Cyanothece* sp. (Bandyopadhyay et al. 2010).

This study describes the relationship between net $H_2$ production and $N_2$ fixation in *T. erythraeum* IMS101. Both net $H_2$ production and $N_2$ fixation varied as a function of the intensity and spectral composition of light. A series of manipulation experiments was used to demonstrate a relationship between the supply of light-derived energy and the electron transport kinetics associated with the level of PQ pool reduction.

## MATERIALS AND METHODS

*Culture conditions.* Cultures of *T. erythraeum* strain IMS101 were grown in 500 mL culture flasks using YBC II (Yi-Bu Chen) medium (pH 8.0 and salinity of 34) (Chen et al. 1996), at 26°C with a 12 h square-wave light:dark (L:D) cycle and a light intensity of 50 μmol photons $\cdot$ $m^{-2}$ $\cdot$ $s^{-1}$. A subculture of *Trichodesmium* was also maintained at 500 μmol photons $\cdot$ $m^{-2}$ $\cdot$ $s^{-1}$ for a period of 5 d using an array of high-intensity blue and green light emitting diodes (LEDs) before conducting light intensity manipulation experiments. The growth of the cultures was monitored daily by measurements of *in vivo* fluorescence using a Turner Designs fluorometer (TD-700, Turner Inc., Sunnyvale, CA, USA). Experiments were always conducted on *Trichodesmium* cultures when they were in exponential growth phase. Furthermore, all the manipulation experiments were conducted at least 3 h after the onset of the light period and 2 h before the dark period. During this timeframe, $C_2H_4$ production, net $H_2$ production, and the variable fluorescence due to endogenous diel rhythms are relatively stable (Fig. 1), and changes in the diazotrophic and photosynthetic activity are considered to be a result of the experimental manipulations.

*Experimental conditions.* The stock cultures were transferred to borosilicate glass vials for experimental manipulation. For each experiment, cultures were analyzed continuously for ethylene ($C_2H_4$) production, net $H_2$ production, and variable fluorescence (as described in the ''Analytical configuration'' section) for up to 6 h. The advantages of having a high-resolution data output are countered by the restriction of analyzing a single subculture for a particular experiment. Therefore, replicate measurements were conducted on separate days using independent cultures. The data presented in the ''Results'' section are representative examples of each experiment with typically a single replicate.

*Analytical configuration.* The suite of analytical measurements included net $H_2$ production, $N_2$ fixation measured by acetylene ($C_2H_2$) reduction, and electron transport kinetics

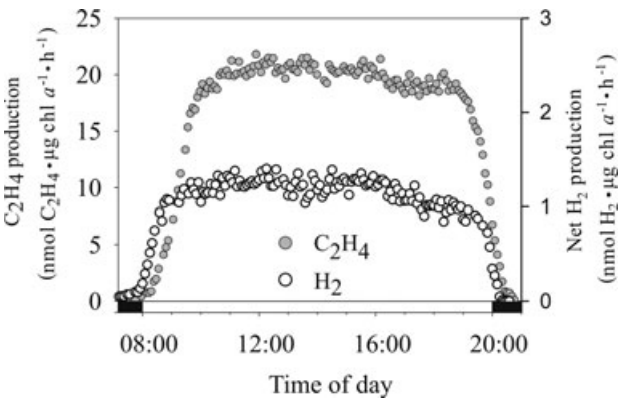


FIG. 1. Diel profile of $C_2H_4$ production and net $H_2$ production by *Trichodesmium* maintained at 26°C and 50 μmol μmol photons $\cdot$ $m^{-2}$ $\cdot$ $s^{-1}$ on a 12:12 light:dark cycle. The manipulation experiments (Figs. 2–7) were conducted between 3 and 9 h into the light period.

measured using FRRF, described in detail below. The analyses ran simultaneously providing online, real-time measurements at 120 and 240 s time intervals for $H_2$ production and $C_2H_2$ reduction, and 10 s intervals for FRRF-based photosynthetic characteristics including the functional absorption cross-section ($\sigma_{PSII}$), the efficiency of charge separation ($\phi_{PSII}$), and the kinetics of photosynthetic electron transport rate (PETR). These experiments extended for periods of a few hours and were always terminated 2 h prior to the onset of the dark period, before $N_2$ fixation begins to decrease. Attention was also paid to ensure identical experimental conditions in $H_2$ production, $N_2$ fixation, and photosynthetic measurements, as each was performed on separate subsamples of the *Trichodesmium* culture. For net $H_2$ production and $C_2H_2$ reduction measurements, a typical volume of 40 mL of *Trichodesmium* culture in a crimp-sealed 76 mL borosilicate glass vial was maintained at 26°C using a heating block and illuminated with an overhead light source consisting of three blue (470 nm) and three green (510 nm) LEDs (Lumileds LXHL-NB98 and LXHL-NM98, respectively, Philips Lumileds, San Jose, CA, USA). The light was redirected toward the side walls of incubation vials with a set of mirrors positioned at 45° from the light source, and the light distribution was measured with a scalar PAR irradiance sensor (QSL-2101; Biospherical Instruments Inc., San Diego, CA, USA). For FRRF, 20 mL of *Trichodesmium* culture in a crimp-sealed 76 mL borosilicate glass vial was incubated under identical light conditions in the sample chamber of the FRRF instrument. Net $H_2$ production was quantified using a reduced gas analyzer (RGA) (Peak Laboratories, Mountain View, CA, USA) as previously described (Wilson et al. 2010a).

Measurements of $C_2H_2$ reduction were made using an online gas chromatography (GC) system (Staal et al. 2001), which incorporated several minor modifications as previously reported (Wilson et al. 2010a). Nitrogenase activity is expressed in terms of $C_2H_4$ production, except when rates of $N_2$ fixation are compared to net $H_2$ production. To convert $C_2H_4$ production rates to $N_2$ fixation, a ratio of 4 mol of $C_2H_4$ produced per mol of $N_2$ reduced was used (Capone 1993). Variable fluorescence was measured using a fourth-generation bench-top FRRF, which measures fluorescence transients induced by a series of subsaturating excitation pulses from a bank of high-intensity LEDs to derive photosynthetic parameters (Kolber et al. 1998). This instrument was modified to operate at excitation wavelengths of 445, 470, 503, and 530 nm (with 20, 25, 30, and 35 nm half bandwidths, respectively) to measure spectrally resolved functional absorption cross-section and to provide spectrally resolved background illumination at these wavelengths. The FRRF was used to determine the photochemical quantum yield ($F_v/F_m$), which is the ratio of the maximum change in variable fluorescence ($F_v$) to the maximum fluorescence yield ($F_m$). This value was determined from the initial dark-adapted fluorescence ($F_o$) and $F_m$ when all PSII reaction centers (RC) are photochemically reduced ($F_v/F_m = (F_m - F_o)/F_m$). The functional absorption cross-section of PSII ($\sigma_{PSII}$) was calculated according to Kolber et al. (1998). The steady-state electron transfer rates were calculated as

$$\mathrm{ETR}(\lambda_e) = E(\lambda_e) \cdot (F_m - F_s)/(F_m - F_o) \cdot \sigma_{PSII}(\lambda_e) \qquad (2)$$

where $\lambda_e$ is the excitation wavelength for both the ambient illumination and for pulsed light used to measure the photosynthetic characteristics. The level of PQ pool reduction was calculated as a function of photochemical quenching

$$\mathrm{qp} = (F_m - F_s)/(F_m - F_o) \qquad (3)$$

based on the empirically derived relationship between the level of QA reduction and PQ pool reduction. Chl *a* concentrations were measured at the beginning of each experiment. Triplicate aliquots of cultures were filtered onto 25 mm GF/F filters (Whatman, USA), and the chl *a* was extracted in 5 mL of 90% acetone for 24 h at −20°C before being analyzed using a Turner Designs Model 10-AU fluorometer (Strickland and Parsons 1972).

*Effects of light intensity.* The effect of short-term changes in light intensity on the relationship between $N_2$ fixation, $H_2$ production, and PQ redox state was investigated by incrementally increasing the ambient light intensity over 10 discrete light levels ranging from 25 to 1,000 μmol photons · $m^{-2}$ · $s^{-1}$. After an initial adjustment period at 25 μmol photons · $m^{-2}$ · $s^{-1}$, which lasted up to 2 h, the light intensity was increased at 30 min intervals. The physiological responses in the net $H_2$ and $C_2H_4$ evolution to increasing light regime were evident within the first 10 min of the irradiance pertubations. The effect of increasing light intensity was also investigated in *Trichodesmium* cultures that have been maintained under an elevated light level of 500 μmol photons · $m^{-2}$ · $s^{-1}$ for a period of 5 d. The physiological status and the extent of photoinhibition in the high-light grown culture were analyzed using FRRF measurements. Subsamples were reverted back to low-light level (50 μmol photons · $m^{-2}$ · $s^{-1}$) on six separate occasions during the diel cycle, which covered both light and dark periods, and the response in $F_v/F_m$ analyzed.

*Effects of spectral composition.* The effect of spectral composition of the ambient light was investigated by alternating between blue light (470 nm, 30 nm half bandwidth) and green light (530 nm, 30 nm half bandwidth). Prior to the experiment, cells were adapted to blue light at 50 μmol photons · $m^{-2}$ · $s^{-1}$ for 2 h. The alternating pattern of blue and green light was applied at 30 min intervals. The light intensity was subsequently increased to 300 μmol photons · $m^{-2}$ · $s^{-1}$ (which exceeds the saturation level of 200 μmol photons · $m^{-2}$ · $s^{-1}$ for $C_2H_4$ production), and again the color of the light was alternated every 30 min between blue and green wavelengths.

*Effects of DCMU addition.* To examine the effect of light on the $H_2$:$N_2$ ratio in absence of PSII activity, the inhibitor DCMU was added to *Trichodesmium* samples maintained at 26°C and 50 μmol photons · $m^{-2}$ · $s^{-1}$. DCMU prevents the flow of electrons from PSII to PQ, disrupting the oxidative water splitting (Bothe and Loos 1972). DCMU was added to a final concentration of 1 μmol · $L^{-1}$, which was confirmed by FRRF to fully block the flow of water-derived photosynthetic electrons to the PQ pool. Two additional manipulation experiments were conducted in the presence of DCMU. In the first experiment, the light was increased to 300 μmol photons · $m^{-2}$ · $s^{-1}$ to examine the effects of light on the rate of $N_2$ fixation in the absence of water-derived electrons. In the second experiment, the $O_2$ was removed from the incubation vessel to investigate the redistribution of organic-carbon-derived electrons between nitrogenase and the terminal cytochrome oxidase. These manipulations also served to confirm that the presence of DCMU at 1 μmol · $L^{-1}$ concentration did not affect cellular metabolism beyond disruption of the photosynthetic electron from water to PQ pool.

*Effects of DBMIB additions.* To further investigate the influence of the redox state of the PQ pool on $N_2$ fixation, the inhibitor DBMIB was added to *Trichodesmium* samples maintained at 26°C under 50 μmol photons · $m^{-2}$ · $s^{-1}$ blue (470 nm, 30 nm half bandwidth) light. DBMIB blocks the transfer of electrons from the PQ pool to cytochrome $b_6/f$ (Eisbrenner and Bothe 1979). The objective was to manipulate the level of PQ pool reduction using varying concentrations of DBMIB while maintaining constant illumination. In the control experiments the FRRF data indicated that 3 μmol · $L^{-1}$ (final concentration) DBMIB was sufficient to fully reduce PQ pool under 50 μmol photons · $m^{-2}$ · $s^{-1}$ of ambient light (data not shown). DBMIB was added at ~30 min intervals in

0.5 μmol $L^{-1}$ increments to a final concentration of 2.5 μmol · $L^{-1}$.

## RESULTS

Cultures of *T. erythraeum* maintained on a 12:12 L:D light regime at 50 μmol photons · $m^{-2}$ · $s^{-1}$ grew at 0.2–0.25 $d^{-1}$. The time series profiles of $C_2H_4$ and net $H_2$ production exhibited distinct diel cycles (Fig. 1). $C_2H_4$ production increased rapidly after the onset of the light period reaching a maximum of 22 ± 5 nmol $C_2H_4$ · μg chl $a^{-1}$ · $h^{-1}$ (mean ± standard deviation [SD] derived from the analysis of three independent cultures) during the middle of the light period. Net $H_2$ production was coincident with $C_2H_4$ production, achieving a maximum rate of 1.2 ± 0.4 nmol $H_2$ · μg chl $a^{-1}$ · $h^{-1}$ (mean ± SD based on the analysis of three independent cultures). Both $C_2H_4$ and net $H_2$ production in *Trichodesmium* were maintained throughout most of the light period, decreasing 1–2 h before the onset of the dark period. During the light period, the photosynthetic quantum yield ($F_v/F_m$) ranged from 0.3 in the cultures maintained at 500 μmol photons · $m^{-2}$ · $s^{-1}$ to 0.58 in cultures grown at 50 μmol photons · $m^{-2}$ · $s^{-1}$.

*Trichodesmium* cultures grown at 50 μmol photons · $m^{-2}$ · $s^{-1}$ displayed two distinct phases in the rate of $C_2H_4$ production in response to increasing light intensity (Fig. 2). At light intensities ranging from 25 to 200 μmol photons · $m^{-2}$ · $s^{-1}$, $C_2H_4$ production increased from 12 to 30 nmol $C_2H_4$ · μg chl $a^{-1}$ · $h^{-1}$. At light intensities in excess of 200 μmol photons · $m^{-2}$ · $s^{-1}$, $C_2H_4$ production stabilized and displayed no further increase. Net $H_2$ production also displayed two distinct phases with response to increasing light intensity. Between 25 and 200 μmol photons · $m^{-2}$ · $s^{-1}$, $H_2$ production increased 4-fold from 0.3 to 1.3 nmol $H_2$ · μg chl $a^{-1}$ · $h^{-1}$. At light intensity exceeding 200 μmol photons · $m^{-2}$ · $s^{-1}$, net $H_2$ production continued to increase, but at a reduced rate, reaching 2.2 nmol $H_2$ · μg chl $a^{-1}$ · $h^{-1}$ at 1,000 μmol photons · $m^{-2}$ · $s^{-1}$. Increasing light intensity also induced a progressive increase in the PQ pool redox state, reaching a maximum of 84% at 1,000 μmol photons · $m^{-2}$ · $s^{-1}$ (Fig. 2b). The electron transport rate reached a maximum of 263 electrons · $RCII^{-1}$ · $s^{-1}$ at 750 μmol photons · $m^{-2}$ · $s^{-1}$ before declining slightly at 1,000 μmol photons · $m^{-2}$ · $s^{-1}$ (Fig. 2b). Overall, the $F_v/F_m$ decreased steadily from 0.57 to 0.16 as the light intensity reached a level of 1,000 μmol photons · $m^{-2}$ · $s^{-1}$ (Fig. 2c).

*Trichodesmium* cultures maintained at 500 μmol photons · $m^{-2}$ · $s^{-1}$ for 5 d displayed a different response to increasing light intensity compared to *Trichodesmium* grown at 50 μmol photons · $m^{-2}$ · $s^{-1}$ (Fig. 3). The light-dependent phase of $C_2H_4$ production extended to 350 μmol photons · $m^{-2}$ · $s^{-1}$ increasing from 12 to 38 nmol $C_2H_4$ · μg chl $a^{-1}$ · $h^{-1}$. Increase in light intensity to 1,000 μmol photons · $m^{-2}$ · $s^{-1}$ further raised $C_2H_4$ production, albeit at smaller rate, from 40 to 42 nmol $C_2H_4$ · μg chl $a^{-1}$ · $h^{-1}$ (Fig. 3a). Net $H_2$ production increased 5-fold from 0.5 to 2.7 nmol $H_2$ · μg chl $a^{-1}$ · $h^{-1}$ between 25 and 1,000 μmol photons · $m^{-2}$ · $s^{-1}$. Increasing light intensity also induced a progressive increase in the PQ pool redox state, reaching a maximum of 86% at 1,000 μmol photons · $m^{-2}$ · $s^{-1}$ (Fig. 3b). The maximum electron transport rate of 378 electrons · $RCII^{-1}$ · $s^{-1}$ occurred at 500 μmol photons · $m^{-2}$ · $s^{-1}$ (Fig. 3b). The $F_v/F_m$ decreased steadily from 0.37 to 0.07 at a light intensity of 1,000 μmol photons · $m^{-2}$ · $s^{-1}$ (Fig. 3c). The photoinhibitory effects resulting from exposure to the high-light intensity were examined using FRRF. After a subsample of the high-light-acclimated culture was placed under a low-light level (50 μmol photons · $m^{-2}$ · $s^{-1}$), the cells displayed 80% recovery from photoinhibition within 120 min (data not shown). Repeated measurements throughout the diel cycle revealed that photoinhibition was most

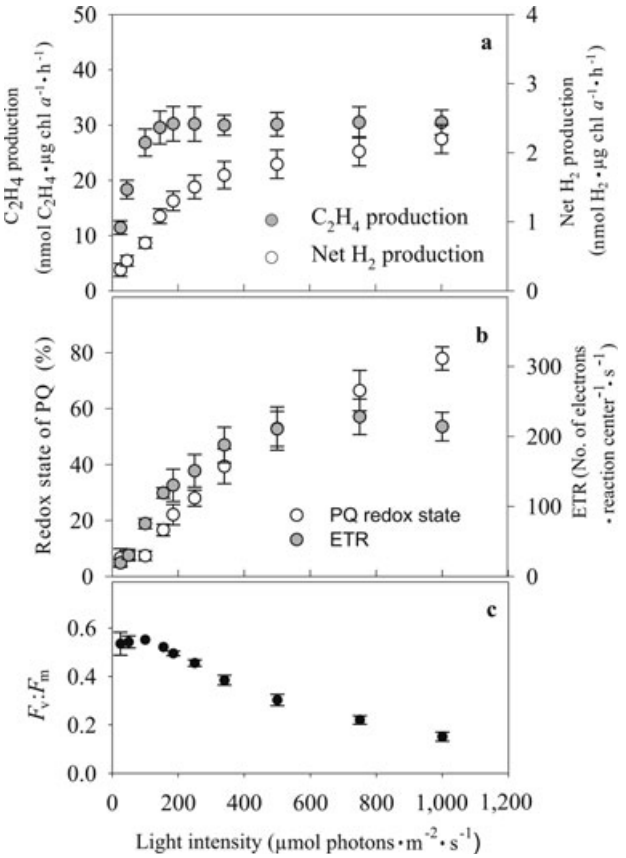


FIG. 2. The influence of light intensity on (a) $C_2H_4$ and net $H_2$ production, (b) the redox state of the plastoquinone pool and the electron transport rate, and (c) $F_v/F_m$, for cultures of *Trichodesmium* maintained at 50 μmol photons · $m^{-2}$ · $s^{-1}$ on a 12:12 light:dark cycle. The error bars represent ±1 SD.

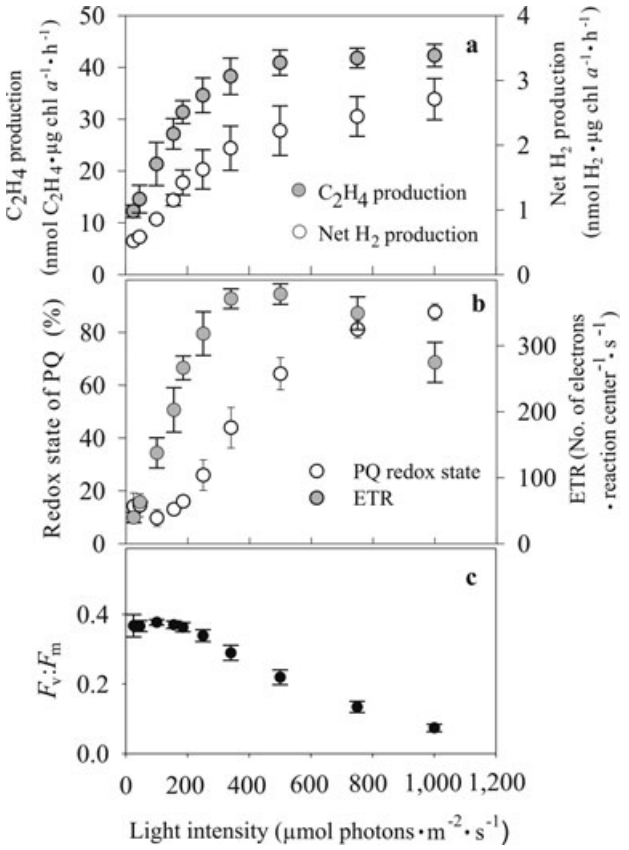


FIG. 3. The influence of light intensity on (a) $C_2H_4$ and net $H_2$ production, (b) the redox state of the plastoquinone pool and the electron transport rate, and (c) $F_v/F_m$, for cultures of *Trichodesmium* that had been exposed to 500 µmol photons · $m^{-2}$ · $s^{-1}$ for a period of 5 d on a 12:12 light:dark cycle. The error bars represent ±1 SD.

pronounced within the first hour of the light period when the $F_v/F_m$ signal was ~60% depressed compared with the dark period.

Alternating the spectral composition between green and blue light affected both $C_2H_4$ and net $H_2$ production and modified the redox state of the PQ pool (Fig. 4). The results from replicating this experiment on a separate occasion are in the supplementary material (Fig. S1). At 100 µmol photons · $m^{-2}$ · $s^{-1}$ of blue light, $C_2H_4$ production reached 23 nmol $C_2H_4$ · µg chl $a^{-1}$ · $h^{-1}$, and $H_2$ production was 0.9 nmol $H_2$ · µg chl $a^{-1}$ · $h^{-1}$. Switching to 100 µmol photons · $m^{-2}$ · $s^{-1}$ of green light induced an increase in $C_2H_4$ production to 26 nmol $C_2H_4$ · µg chl $a^{-1}$ · $h^{-1}$ and an increase in $H_2$ production to 1.3 nmol $H_2$ · µg chl $a^{-1}$ · $h^{-1}$. This pattern was consistently observed during several cycles of alternating between blue and green light. During the third ''blue light'' period (Fig. 4), the light intensity was raised to 300 µmol photons · $m^{-2}$ · $s^{-1}$, which caused an increase in $C_2H_4$ production to 30 nmol $C_2H_4$ · µg chl $a^{-1}$ · $h^{-1}$ and an increase in $H_2$ production to 1.6 nmol $H_2$ · µg chl $a^{-1}$ · $h^{-1}$. The differences in $C_2H_4$ production were minimal between blue and green light at 300 µmol photons · $m^{-2}$ · $s^{-1}$. However, net $H_2$ production still displayed oscillation with an amplitude of 0.3–1.9 nmol $H_2$ · µg chl $a^{-1}$ · $h^{-1}$ when changing light color.

The addition of DCMU had a negative effect on the rate of $C_2H_4$ and net $H_2$ production in *Trichodesmium*. Under a light intensity of 50 µmol photons · $m^{-2}$ · $s^{-1}$, the initial level of $C_2H_4$ production following the addition of DCMU (Fig. 5) remained constant for ~10 min and then decreased steadily during the next 60 min from 12 to 4 nmol $C_2H_4$ · µg chl $a^{-1}$ · $h^{-1}$. The increase in light intensity to 300 µmol photons · $m^{-2}$ · $s^{-1}$ (Fig. 5) temporarily increased $C_2H_4$ production by ~20%, which subsequently stabilized at 4 nmol $C_2H_4$ · µg chl $a^{-1}$ · $h^{-1}$ for 90 min. After this period, $C_2H_4$ production resumed its downward trend and completely ceased 3 h after the addition of DCMU to the culture. Net $H_2$ production declined faster than $C_2H_4$ production, reaching near-zero values within 90 min after DCMU addition, when $C_2H_4$ production was still at 35% of its initial value (Fig. 5, b and d). The change in light intensity from 50 to 300 µmol photons · $m^{-2}$ · $s^{-1}$ had no effect on net $H_2$ production, despite the increased rates of $C_2H_4$ production. Replicate analysis of the DCMU-manipulation experiments on independent cultures also showed a temporary increase in $C_2H_4$ production in response to an increasing light level. However, in this instance, the increase was more transient, lasting ~30 min before resuming its downward trend (Fig. 5c).

A similar pattern of a transient increase in $C_2H_4$ production in the presence of DCMU was observed after removing the $O_2$ from the incubation vessel (Fig. 6), causing an almost 2-fold increase in $C_2H_4$ production before it resumed a gradual decline. The rate of this decline was slowed 3-fold compared to aerobic conditions, reaching a final concentration of 2.9 nmol $C_2H_4$ · µg chl $a^{-1}$ · $h^{-1}$ before the lights were switched off and $C_2H_4$ production was terminated (Fig. 6a). A repeat of the experiment saw an increase in $C_2H_4$ production and a subsequent stabilization before the lights were switched off (Fig. 6c). Once again, no net $H_2$ production was observed during the transient increase in $C_2H_4$ production in response to aerobic conditions.

The artificial manipulation of the PQ redox state by the incremental addition of 0.5 µM DBMIB aliquots under 50 µmol photons · $m^{-2}$ · $s^{-1}$ affected both $C_2H_4$ and net $H_2$ production (Fig. 7). The results from replicating this experiment on a separate occasion are in the supplementary material (Fig. S2). With DBMIB concentrations increasing to 1.0 µM and the level of PQ pool reduction reaching 50%, the $C_2H_4$ production decreased from an initial level of 13 nmol $C_2H_4$ · µg chl $a^{-1}$ · $h^{-1}$ to 10 nmol $C_2H_4$ · µg chl $a^{-1}$ · $h^{-1}$ while the net $H_2$ production increased from 0.8 to 0.94 nmol $H_2$ µg chl $a^{-1}$ $h^{-1}$,

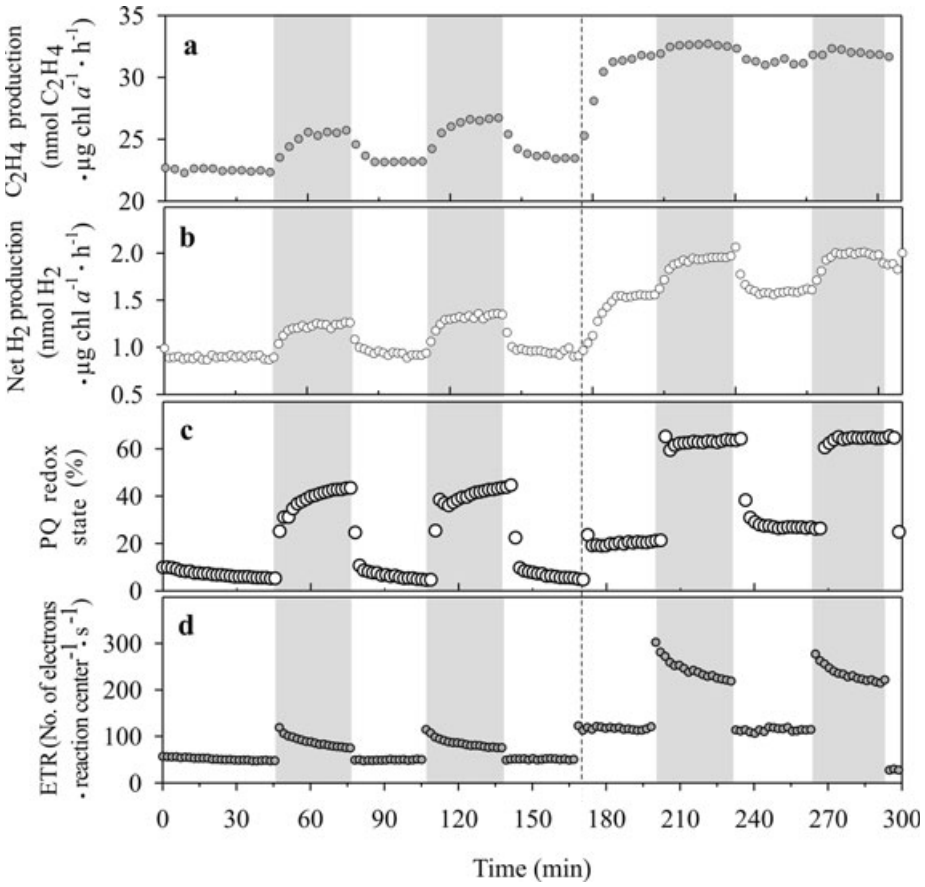


FIG. 4. Effect of altering the spectral quality on (a) $C_2H_4$ production, (b) net $H_2$ production, (c) the redox state of the plastoquinone pool, and (d) the electron transport rate, for *Trichodesmium*. The shaded boxes indicate when the cells were exposed to green light (512 nm). At all other times, the cells were maintained under blue light (470 nm). The time point when the light intensity is increased from 100 to 300 μmol photons · $m^{-2}$ · $s^{-1}$ is indicated by the dashed line.

in proportion to the level of PQ pool reduction. The subsequent increases in DBMIB concentration further reduced the PQ pool to 70% and caused a continual decrease in $C_2H_4$ production but reversed the trend of net $H_2$ production.

## DISCUSSION

The $H_2$:$N_2$ ratio can be interpreted as a measure of the metabolic efficiency associated with nitrogenase activity (Schubert and Evans 1976). In laboratory cultures of *Trichodesmium*, maintained at 26°C and 50 μmol photons · $m^{-2}$ · $s^{-1}$, the $H_2$:$N_2$ ratio ranges from 0.2 to 0.3 (Fig. 1), which is comparable to values measured for heterocystous cyanobacteria (Masukawa et al. 2001), but two orders of magnitude greater than observed in unicellular cyanobacterium *Crocosphaera watsonii* (Wilson et al. 2010b). We hypothesize that the difference between the $H_2$:$N_2$ ratios associated with *crocosphaera* and *Trichodesmium* reflects the availability of light-derived energy during the time frame when nitrogenase is active. When photosynthesis and $N_2$ fixation overlap on a temporal basis, there is less demand for the electrons resulting from $H_2$ oxidation, causing greater net $H_2$ production and therefore a higher $H_2$:$N_2$ ratio. A series of short-term manipulation experiments revealed the relationship between $H_2$ production and $N_2$ fixation as it relates to the cycling of electrons through the PQ pool in *Trichodesmium*.

*Effect of light intensity on $C_2H_4$ production and net $H_2$ production.* The patterns of diazotrophic responses to light in *Trichodesmium* are strongly controlled by the growth irradiance regime. In cells grown at 50 μmol photons · $m^{-2}$ · $s^{-1}$, nitrogenase activity saturates at 200 μmol photons · $m^{-2}$ · $s^{-1}$. This value is slightly higher than that previously observed for different strains of *Trichodesmium* (e.g., Ohki and Fujita 1988, Bell and Fu 2005). An increase in growth irradiance to 500 μmol photons · $m^{-2}$ · $s^{-1}$ shifts the saturation level beyond this level within just few days of high-light acclimation (Fig. 3a). The saturation of nitrogenase activity prior to the saturation of photosynthetic electron transport (Fig. 2a) has been attributed to the inhibition of nitrogenase by $O_2$

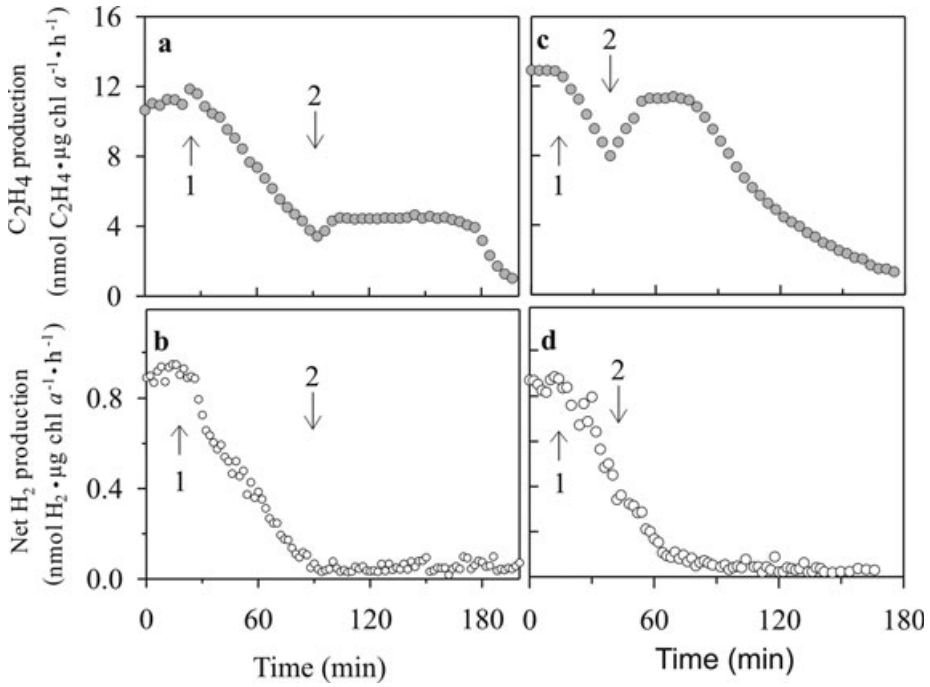


FIG. 5. Effect of DCMU (final concentration 1 µmol · $L^{-1}$) on (a) $C_2H_4$ production and (b) net $H_2$ production by *Trichodesmium*. The addition of DCMU is highlighted (arrow 1) and the light intensity was increased from 50 to 300 µmol photons · $m^{-2}$ · $s^{-1}$ after 90 min (arrow 2). This experiment was repeated using an independent culture of *Trichodesmium* on a separate occasion as shown by (c) $C_2H_4$ production and (d) net $H_2$ production. DCMU, 3-(3,4-dichlorophenyl)-1,1-dimethylurea.

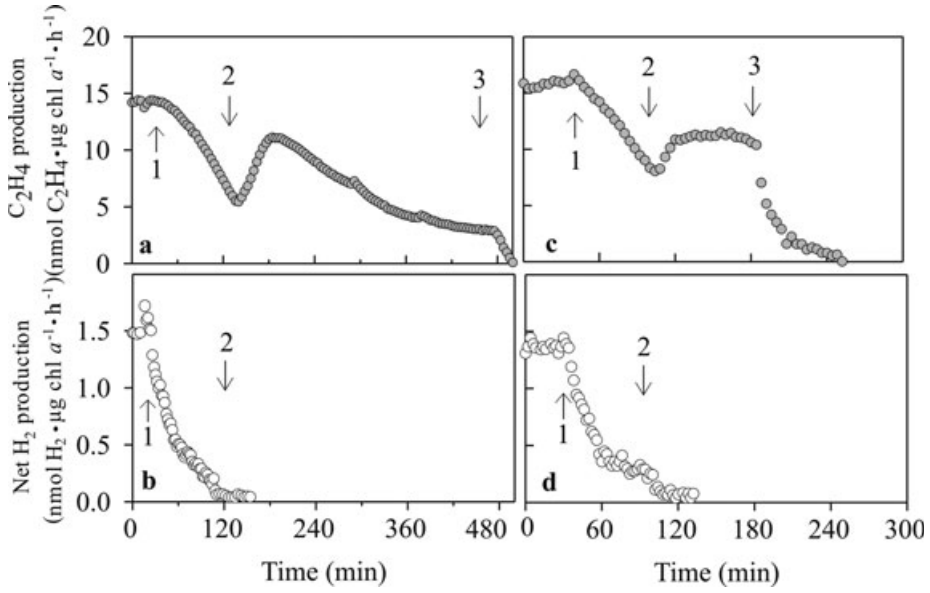


FIG. 6. Effect of DCMU (final concentration 1 µmol · $L^{-1}$) on (a) $C_2H_4$ production and (b) net $H_2$ production by *Trichodesmium*. The addition of DCMU (arrow 1), the removal of $O_2$ supply (arrow 2), and switching off the lights (arrow 3) are highlighted. This experiment was repeated using an independent culture of *Trichodesmium* on a separate occasion as shown by (c) $C_2H_4$ production and (d) net $H_2$ production. DCMU, 3-(3,4-dichlorophenyl)-1,1-dimethylurea.

resulting from increased photosynthetic activity at high-light levels (Paerl 1994). Herein we show that nitrogenase can respond to a 44% increase in the electron transport rate (Fig. 3b) in cells acclimated to higher light levels. The higher rate of nitrogenase activity appears to correlate with the higher turnover rate of photosynthetic electron transport. In addition to elevated rates of the linear and cyclic

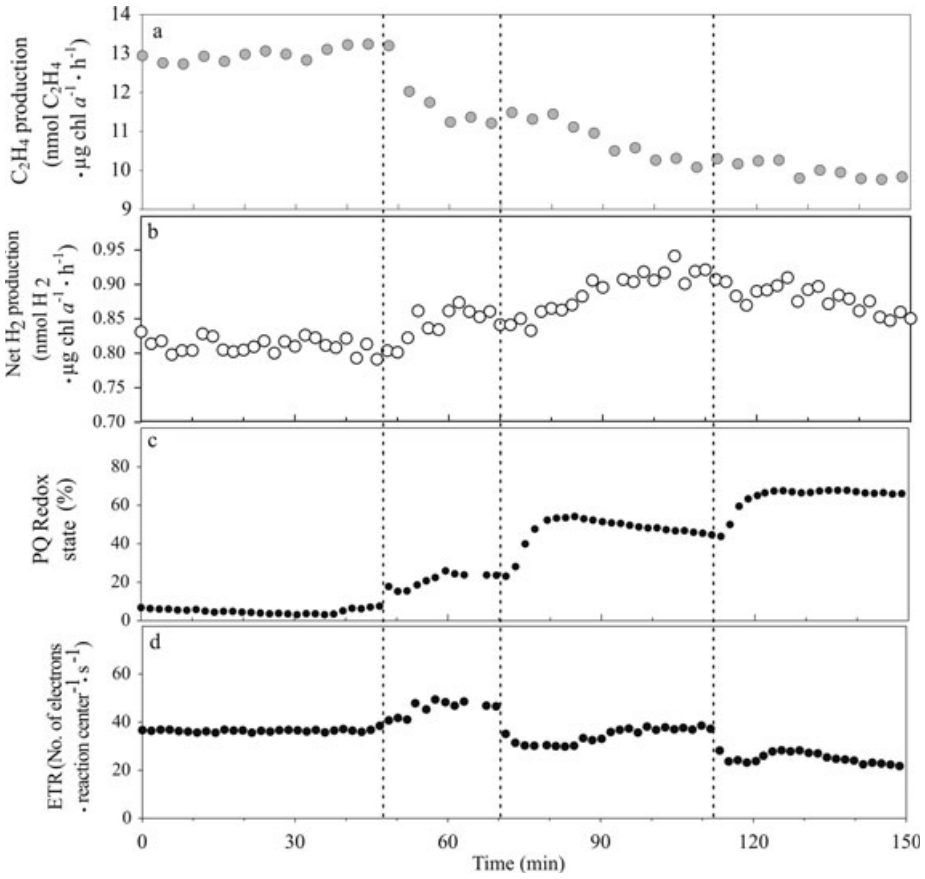


FIG. 7. Effect of incremental additions of the inhibitor DBMIB (0.5 µmol · $L^{-1}$) on (a) $C_2H_4$ production, (b) $H_2$ production, (c) the redox state of the plastoquinone pool, and (d) the electron transport rate, for *Trichodesmium*. The dashed lines indicate the time points when DBMIB was added. DBMIB, 2,5-dibromo-3-methyl-6-isopropyl-p-benzoquinone.

electron transport, this may also reflect increased activity of the Mehler reaction, where the water-derived electrons are used to reduce $O_2$ at the acceptor side of PSI, thus alleviating the negative effects of increased $O_2$ production at the water-splitting site of PSII (Kana 1993). It has previously been shown that *Trichodesmium* grown at 200 µmol photons · $m^{-2}$ · $s^{-1}$ has $O_2$ uptake rates 2- to 3-fold higher than *Trichodesmium* cells grown at 50 µmol photons · $m^{-2}$ · $s^{-1}$ (Kranz et al. 2010).

Both the low-light- and the high-light-grown cultures of *Trichodesmium* displayed two phases of $C_2H_4$ production and the net production of $H_2$ as a function of light intensity. This two-phase pattern was most pronounced in the low-light-grown culture, with the $C_2H_4$ production saturating completely at a 200 µmol photons · $m^{-2}$ · $s^{-1}$. Although the slope of the net production of $H_2$ changed abruptly at this light level, $H_2$ production continued to rise as the light increased to 1,000 µmol photons · $m^{-2}$ · $s^{-1}$ (Fig. 2a). The continuing increase in net $H_2$ production under conditions of leveled nitrogenase activity may be attributed to a decrease in the reassimilation of $H_2$, coinciding with an increase in PQ reduction (Fig. 2b). This may indicate that net $H_2$ production is affected by the redox state of the PQ pool, whereby the ability of the PQ pool to accept $H_2$-derived electrons from uptake hydrogenase decreases as it becomes progressively reduced. A similar pattern is observed in the high-light-grown cells, although in this case the saturation level of nitrogenase activity, and the corresponding change in the slope of $H_2$ production, shifts to ~350 µmol photons · $m^{-2}$ · $s^{-1}$.

*Effect of spectral irradiance on net $H_2$ production.* The effect of light was further demonstrated by varying the spectral composition of ambient light. At 100 µmol photons · $m^{-2}$ · $s^{-1}$ when nitrogenase activity is light limited, switching from blue to green light resulted in an increased $C_2H_4$ production (Fig. 4a). This increase is due to the differences in light-harvesting ability of *Trichodesmium*-specific photosynthetic pigments at different wavelengths. Green light is absorbed specifically by phycoerythrin with high efficiency of excitation capture and transfer from phycobilisomes to PSII and PSI (Campbell 1996). Blue light is predominantly absorbed by chl *a*, which constitutes only a small fraction of the light-harvesting pigments in *Trichodesmium* (Stanier and Cohen-Bazire 1977). The functional absorption

cross-section measured under blue light $\sigma_{PSII}(470)$ averaged $\sim 105\ Å^2 \cdot q^{-1}$, and under green light $\sigma_{PSII}(530)$ averaged at $\sim 200\ Å^2 \cdot q^{-1}$. As the blue light at 100 μmol photons $\cdot\ m^{-2} \cdot s^{-1}$ is insufficient to saturate nitrogenase activity, switching from blue to green light at this light level increases rates of both the $C_2H_4$ production and $H_2$ production by a fraction roughly proportional to the $\sigma_{PSII}(530)/\sigma_{PSII}(470)$.

In contrast, at 300 μmol photons $\cdot\ m^{-2} \cdot s^{-1}$ the switch from blue light to green light has no effect on $C_2H_4$ production by *Trichodesmium* due to the fact that nitrogenase activity is already saturated under the blue light. However, switching from blue to green light at 300 μmol photons $\cdot\ m^{-2} \cdot s^{-1}$ increased the level of PQ pool reduction by 2-fold (Fig. 4c) due to the higher flux of photosynthetic electrons (Fig 4d) with concomitant increase in the net $H_2$ production (Fig. 4b). The higher level of PQ pool reduction under these conditions is likely to decrease the ability of PQ pool to accept electron from the uptake hydrogenase resulting in higher rates of $H_2$ lost to the environment.

In addition to the importance of $H_2$ cycling at the cellular level, the cycling of $H_2$ can also be considered in relation to $N_2$ fixation in the marine environment. The results from the spectral manipulation experiments indicate that the rates of net $H_2$ production by *Trichodesmium* within the upper water column (0–75 m) may be elevated relative to $N_2$ fixation as a result of both the higher light intensity and the greater contribution of longer wavelengths (green light) of the available light. At the moment, there is only limited evidence from the field-based measurements of either dissolved $H_2$ concentrations or $N_2$ fixation in open-ocean surface seawater to support this hypothesis. Depth profiles of $N_2$ fixation, as measured by $^{15}N_2$ assimilation, at Station ALOHA (22° 45′ N, 158 °W) frequently show a decrease in $^{15}N_2$ assimilation rates at a depth 75 m (Church et al. 2009) where light levels are $\sim$70 μmol photons $\cdot\ m^{-2} \cdot s^{-1}$. It remains to be seen whether the decrease in $N_2$ fixation at this depth results from light limitation of nitrogenase as indicated by the findings of our study. Furthermore, vertical profiles of dissolved $H_2$ concentrations (e.g., Conrad and Seiler 1988) do not reveal a consistent increase from a depth of 75 m toward the surface. However, it should also be noted that an absence of any gradient in $H_2$ concentrations in the upper 75 m might also result from the rate of $H_2$ turnover increasing proportional to the rate of $H_2$ production (Conrad 1988), and to our knowledge, rates of $H_2$ consumption have not been measured in the open ocean.

*Net $H_2$ production and $N_2$ fixation during limited supply of water-derived electrons.* The ability of *Trichodesmium* to fix $N_2$ during daylight provides nitrogenase with both photosynthetic and respiratory-derived electrons and energy. However, to protect the nitrogenase from the adverse effects of photosynthesis-derived $O_2$, a large portion of the photosynthetically produced electrons are utilized to reduce $O_2$ in a Mehler reaction (Kana 1993, Berman-Frank et al. 2001, Milligan et al. 2007). On the other hand, electrons derived from the oxidation of organic carbon are available without any associated ''$O_2$ contamination.'' Respiratory-driven $N_2$ fixation has been reported previously (Ohki and Fujita 1988), and its persistence appears to be extended under anaerobic conditions (Berman-Frank et al. 2001, and this study). As light is required to sustain $N_2$ fixation in *Trichodesmium* cells, respiratory electrons are driven from PQ pool to ferredoxin by the photosynthetic activity of PSI to provide the reducing power required for nitrogenase activity (Fig. 8). A fraction of these electrons may also be recycled around PSI to satisfy the substantial energy requirements of $N_2$ fixation. The gradual decrease in $C_2H_4$ production in the presence of DCMU reflects the progressive depletion of the pool of respiratory electrons toward $N_2$ reduction. This depletion will also degrade the ability of PSI to support the energy requirements for $C_2H_4$ production. These two effects will eventually bring $N_2$ fixation to an end within a time frame defined by the capacity of the respiratory electron pool and by the current rate of $N_2$ fixation, which in turn is influenced by the irradiance level. The transient surge observed in $C_2H_4$ production following the increase in light intensity (Fig. 5, a and c) may reflect nitrogenase response to higher energy flux due to a faster turnover of the remaining respiratory electron pool around PSI under elevated light levels of 300 μmol photons $\cdot\ m^{-2} \cdot s^{-1}$. In addition, a higher light level is likely to produce a more oxidized condition at the donor side of PSI, diverting some of the respiratory electrons from the terminal cytochrome oxidase pathway toward the PSI-ferredoxin-nitrogenase pathway, satisfying the increased demand for reducing equivalents (Fig. 8). The redirection of electrons from cytochrome oxidase to nitrogenase also explains the transient increase that was observed in $C_2H_4$ production following removal of $O_2$ in the presence of DCMU (Fig. 6a). Switching off the light resulted in an immediate termination of $C_2H_4$ production revealing that respiratory electrons enter the ferredoxin-nitrogenase pathway via light-driven action of PSI.

Although the level of PQ pool reduction cannot be monitored in presence of DCMU using FRRF, we assume that it remains low due to an absence of electron flux from PSII. According to our previous observations concerning the PQ redox state and net $H_2$ production (Fig. 2), these conditions should promote effective utilization of electrons from the uptake hydrogenase. Indeed, the net $H_2$ production relative to $C_2H_4$ production decreased progressively in presence of DCMU, ceasing 110 min prior to cessation of $C_2H_4$ production (Fig. 5b), supporting this notion. Furthermore, the increase in light levels

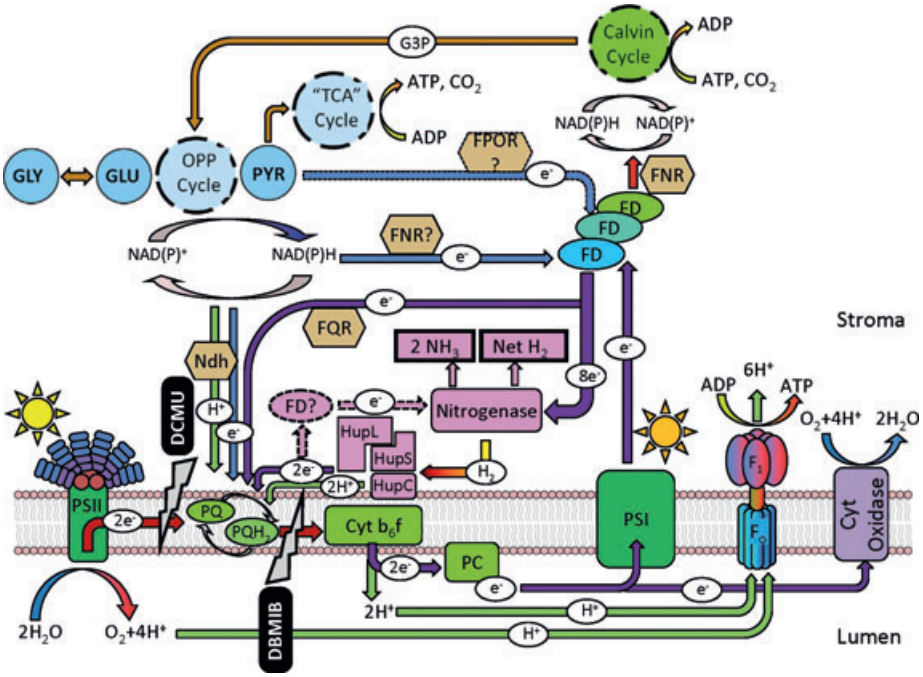


FIG. 8. Photosynthetic and respiratory electron transport pathways relevant for $N_2$ fixation and $H_2$ evolution in *Trichodesmium erythraeum*. Light-driven charge separation in PSII results in oxidation of water and subsequent reduction of plastoquinone (PQ) pool ($PQ \rightarrow PQH_2$). PQ pool is reoxidized by cytochrome $b_6/f$ (Cyt $b_6/f$), transferring the electrons to PSI via plastocyanine (PC), where a second light-driven mechanism transfers the electrons to ferredoxin (FD), initiating NAD(P) reduction by ferredoxin:NAD(P) oxidoreductase (FNR). Water-derived protons accumulating in the lumen activate ATP synthetase ($F_oF_1$), and the acquired reducing equivalents and ATP drive carbon fixation in the Calvin cycle. The product of the carbon fixation, glyceraldehyde-3-phosphate (G3P), enters the oxidative pentose phosphate (OPP) cycle branching to the carbon storage and carbon metabolism pathways. The reducing equivalents extracted from OPP cycle by NAD(P)H enter the PQ pool cycle by the action of NAD(P) dehydrogenase (Ndh), contributing to both photosynthetic electron transport via PSI and to respiratory electron transport terminating on cytochrome oxidase. A fraction of the reduced ferredoxin pool recirculates its electrons back into the PQ pool by the action of ferredoxin:quinone oxireductase (FQR) in a process of light-driven cyclic electron transport around PSI, while shuffling the protons from the stroma back into the lumen, reenergizing the ATP-producing machinery. Another fraction of the reduced ferredoxin supports nitrogenase activity by supplying electrons to the Fe protein of the nitrogenase complex. The evolved hydrogen is oxidized by the uptake hydrogenase (HupL, HupS, and HupC), with electrons reintroduced to the PSI-driven electron transport chain, and the protons transferred to lumen, resupplying the reducing power and energy. DCMU blocks the flow of water-derived electrons into PQ pool and eliminates PSII contribution to ATP generation but does not interrupt the flow of respiratory electrons. DBMIB blocks the reoxidation of the PQ pool, interrupting both the photosynthetic and the respiratory electron flow. DBMIB, 2,5-dibromo-3-methyl-6-isopropyl-p-benzoquinone; DCMU, 3-(3,4-dichlorophenyl)-1,1-dimethylurea.

after 90 min did not produce a corresponding increase in $H_2$ production (Fig. 5, b and d), which usually accompanies changes in the level of $C_2H_4$ production. We hypothesize that the increased demand for the electrons by nitrogenase, combined with decreasing pool of respiratory electrons, poises the PQ pool at an oxidized state, which is indicative of a shortage of reducing power and/or energy at the acceptor side of PSI. These conditions raise the overall efficiency of $H_2$ utilization with the consequence of little or no net $H_2$ production being observed. Nevertheless, a complete cessation of the net $H_2$ production under conditions of still-present $C_2H_4$ production, and lack of $H_2$ response to transient stimulation of $C_2H_4$ production by increased light intensity (Fig. 5) or removal of oxygen (Fig. 6) raises the question of whether the PQ pool is the sole acceptor for the hydrogenase-produced hydrogen. It is also necessary to remember that the cultures were not axenic, and an additional microbial sink for the dissolved $H_2$ may have been opportunistic $H_2$-oxidizing bacteria.

*Effects of DBMIB-modulated changes of PQ redox state on net $H_2$ production.* A different outcome to that obtained with DCMU addition was observed in the presence of DBMIB. The gradual addition of DBMIB caused a progressive reduction of the PQ pool under constant irradiance level, resulting in a proportional decline in the supply of electrons to the acceptor side of PSI, negatively affecting both the cyclic electron transport around PSI (whether fueled by the water-derived, or respiratory-derived, electrons) and the supply of electrons to ferredoxin-nitrogenase pathway (Fig. 8). The diminishing energy production coupled with lower flux of reducing equivalents explains the decline in $C_2H_4$ production. At the same time, as the PQ pool became progressively reduced, its ability to accept electrons from uptake hydrogenase decreases, resulting in a transient increase in net $H_2$ production. This trend,

consistent with all the previous observations, reversed when inhibitor concentrations exceeded 1 $\mu mol \cdot L^{-1}$ and the PQ pool reduction level reached 40% to 50% (Fig. 7b). Additional PQ pool reduction above this level caused a decrease in net $H_2$ production concomitant with the decrease in $C_2H_4$ production. The decrease in net $H_2$ production as a function of DBMIB-induced PQ pool reduction can be explained by the fact that the net $H_2$ production is controlled by both the nitrogenase-driven production of $H_2$ and its assimilation by the uptake hydrogenase. During the first phase of the experiment, the decrease in assimilation rates exceeds the loss of production, resulting in a transient increase of the net $H_2$ production. At increasing concentrations of DBMIB an overall decline in the net $H_2$ level is observed as a result of decreasing net $H_2$ production due to decreased nitrogenase activity.

## CONCLUSIONS

Our observations reveal a clear relationship between $H_2$ production, $N_2$ fixation, and the level of PQ pool reduction in *Trichodesmium*. They also demonstrate that in *Trichodesmium* the $N_2$-fixation process can operate exclusively using the respiratory electrons in the presence of DCMU but requires light to move them along the PSI-ferredoxin pathway. When both PSII and PSI are fully engaged in the light, the flux of water-derived photosynthetic electrons continuously replenishes the pools of respiratory carbon via the process of carbon fixation (Fig. 8) even though a significant fraction of these electrons may be dissipated in $O_2$-consuming Mehler reaction (Berman-Frank et al. 2001). We hypothesize that the relatively high $H_2$:$N_2$ ratio observed in *Trichodesmium* is a measure of an excess of reducing equivalents relative to nitrogenase requirements that can be released without adversely affecting nitrogenase activity under conditions of continuous electron supply from photosynthesis. The excess of reducing power becomes increasingly pronounced at irradiance levels above of ~200 $\mu mol\ photons \cdot m^{-2} \cdot s^{-1}$ (Ohki and Fujita 1988, Bell and Fu 2005, this study). The bidirectional hydrogenase enzyme has been shown to act as an electron release valve during photosynthesis in the cyanobacterium *Synechocystis* (Appel et al. 2000). Although the biological production of $H_2$ has long been recognized as a biochemical mechanism to regulate electron flow and release ''excess'' electrons in anaerobic microorganisms (Gray and Gest 1965), the relatively high level of $H_2$ production observed in this study as compared with *Crocosphaera* (Wilson et al. 2010b) may indicate that the nitrogenase requirements for the reducing power are fully satisfied under normal physiological conditions. These conditions change dramatically following addition of DCMU, where progressive shortage of reducing power induces more efficient reutilization of the nitrogenase-produced electrons. It remains to be resolved what metabolic pathways are involved in this process and what factors control these pathways. It is possible that the activity of the uptake hydrogenase may be up-regulated under conditions of electron shortage. Alternatively, the mechanisms of proton binding and $H_2$ release from nitrogenase may change under condition of progressively oxidized Fe protein or the nitrogenase-serving ferredoxin.

We thank Shellie Bench, Mary Hogan, and Marnie Jo Zirbel for laboratory assistance with the cultures of *Trichodesmium*. We also thank Jim Tripp for constructive discussion and comments. This research was supported by the Gordon and Betty Moore Foundation and the National Science Foundation supported Center for Microbial Oceanography: Research and Education (C-MORE) (EF0424599).

Allahverdiyeva, A., Leino, H., Saari, L., Fewer, D. P., Shunmugam, S., Sivonen, K. & Aro, E.-M. 2010. Screening for biohydrogen production by cyanobacteria isolated from the Baltic Sea and Finnish lakes. *Int. J. Hydrogen Energy* 35:1117–27.

Appel, J., Phunpruch, S., Steinmüller, K. & Schulz, R. 2000. The bidirectional hydrogenase of *Synechocystis* sp. PCC6803 works as an electron valve during photosynthesis. *Arch. Microbiol.* 173:333–8.

Bandyopadhyay, A., Stöckel, J., Min, H., Sherman, L. A. & Pakrasi, H. B. 2010. High rates of photobiological $H_2$ production by a cyanobacterium under aerobic conditions. *Nat. Commun.* 1:139.

Bell, P. R. F. & Fu, F.-X. 2005. Effect of light on growth, pigmentation and $N_2$ fixation of cultured *Trichodesmium* sp. from the Great Barrier Reef lagoon. *Hydrobiologia* 543:25–35.

Berman-Frank, I., Lundgren, P., Chen, Y.-B., Küpper, H., Kolber, Z., Bergman, B. & Falkowski, P. 2001. Segregation of nitrogen fixation and oxygenic photosynthesis in the marine cyanobacterium *Trichodesmium*. *Science* 294:1534–7.

Berman-Frank, I., Quigg, A., Finkel, Z. V., Irwin, A. J. & Haramaty, L. 2007. Nitrogen-fixation strategies and Fe requirements in cyanobacteria. *Limnol. Oceanogr.* 52:2260–9.

Bothe, H. & Loos, E. 1972. Effect of far red light and inhibitors on nitrogen fixation and photosynthesis in the blue-green alga *Anabaena cylindrica*. *Arch. Microbiol.* 86:241–54.

Bothe, H., Neuer, G., Kalbe, I. & Eisbrenner, G. 1980. Electron donors and hydrogenase in nitrogen-fixing microorganisms. *In* Stewart, W. D. P. & Gallon, J. R. [Eds.] *Nitrogen Fixation*. Academic Press, London, pp. 83–112.

Campbell, D. 1996. Complementary chromatic adaptation alters photosynthetic strategies in the cyanobacterium *Calothrix*. *Microbiology* 142:1255–63.

Capone, D. G. 1993. Determination of nitrogenase activity in aquatic samples using the acetylene reduction procedure. *In* Kemp, P. F., Sherr, B. F., Sherr, E. B. & Cole, J. J. [Eds.] *Handbook of Methods in Aquatic Microbial Ecology*. Lewis Publishers, Boca Raton, Florida, pp. 621–31.

Capone, D. G., Zehr, J. P., Paerl, H. W., Bergman, B. & Carpenter, E. J. 1997. *Trichodesmium*, a globally significant marine cyanobacterium. *Science* 276:1221–9.

Chen, Y.-B., Zehr, J. P. & Mellon, M. 1996. Growth and nitrogen fixation of the diazotrophic filamentous nonheterocystous cyanobacterium *Trichodesmium* sp. IMS101 in defined media: evidence for a circadian rhythm. *J. Phycol.* 32:916–23.

Church, M. J., Mahaffey, C., Letelier, R. M., Lukas, R., Zehr, J. P. & Karl, D. M. 2009. Physical forcing of nitrogen fixation and diazotroph community structure in the North Pacific subtropical gyre. *Global Biogeochem. Cycles* 23:GB2020.

Conrad, R. 1988. Biogeochemistry and ecophysiology of atmospheric CO and $H_2$. *Adv. Microb. Ecol.* 10:231–83.

Conrad, R. & Seiler, W. 1988. Methane and hydrogen in seawater (Atlantic Ocean). *Deep-Sea Res.* 35:1903–17.

Dugdale, R. C. & Goering, J. J. 1967. Uptake of new and regenerated forms of nitrogen in primary productivity. *Limnol. Oceanogr.* 12:196–206.

Eisbrenner, G. & Bothe, H. 1979. Modes of electron transfer from molecular hydrogen in *Anabaena cylindrica*. *Arch. Microbiol.* 123:37–45.

Gray, C. T. & Gest, H. 1965. Biological formation of molecular hydrogen. *Science* 148:186–92.

Kana, T. M. 1993. Rapid oxygen cycling in *Trichodesmium thiebautii*. *Limnol. Oceanogr.* 38:18–24.

Karl, D. M. 2007. Microbial oceanography: paradigms, processes and promise. *Nat. Rev. Microbiol.* 5:759–69.

Kolber, Z., Prasÿil, O. & Falkowski, P. G. 1998. Measurements of variable chlorophyll fluorescence using fast repetition rate techniques: defining methodology and experimental protocols. *Biochim. Biophys. Acta* 1367:88–106.

Kranz, S. A., Levitan, O., Richter, K.-U., Prášil, O., Berman-Frank, I. & Rost, B. 2010. Combined effects of $CO_2$ and light in the $N_2$-fixing cyanobacterium *Trichodesmium* IMS101: physiological responses. *Plant Physiol.* 154:334–45.

Lowe, D. J. & Thorneley, R. N. F. 1984. The mechanism of *Klebsiella pneumoniae* nitrogenase action. *J. Biochem.* 224:877–909.

Masukawa, H., Nakamura, K., Mochimaru, M. & Sakurai, H. 2001. Photobiological hydrogen production and nitrogenase activity in some heterocystous cyanobacteria. *In* Miyake, J., Matsunaga, T. & San Pietro, A. [Eds.] *Biohydrogen II.* Elsevier Science, Oxford, UK, pp. 63–6.

Milligan, A. J., Berman-Frank, I., Gerchman, Y., Dismukes, G. C. & Falkowski, P. G. 2007. Light-dependent oxygen consumption in nitrogen-fixing cyanobacteria plays a key role in nitrogenase protection. *J. Phycol.* 43:845–52.

Moore, R. M., Punshon, S., Mahaffey, C. & Karl, D. M. 2009. The relationship between dissolved hydrogen and nitrogen fixation in ocean waters. *Deep-Sea Res.* 56:1449–58.

Ohki, K. & Fujita, Y. 1988. Aerobic nitrogenase activity measured as acetylene reduction in the marine non-heterocystous cyanobacterium *Trichodesmium* spp. grown under artificial conditions. *Mar. Biol.* 98:111–4.

Paerl, H. W. 1994. Spatial segregation of $CO_2$ fixation in *Trichodesmium* spp.: linkage to $N_2$ fixation potential. *J. Phycol.* 30:790–9.

Postgate, J. R. 1982. *The Fundamentals of Nitrogen Fixation.* Cambridge University Press, Cambridge, UK, 252 pp.

Punshon, S. & Moore, R. M. 2008. Aerobic hydrogen production and dinitrogen fixation in the marine cyanobacterium *Trichodesmium erythraeum* IMS101. *Limnol. Oceanogr.* 53:2749–53.

Saino, T. & Hattori, A. 1982. Aerobic nitrogen fixation by the marine non-heterocystous cyanobacterium *Trichodesmium* (*Oscillatoria*) spp.: its protective mechanism against oxygen. *Mar. Biol.* 70:251–4.

Schubert, K. R. & Evans, H. J. 1976. Hydrogen evolution: a major factor affecting the efficiency of nitrogen fixation in nodulated symbionts. *Proc. Natl. Acad. Sci. U. S. A.* 73:1207–11.

Schütz, K., Happe, T., Troshina, O., Lindblad, P., Leitão, E., Oliveira, P. & Tamagnini, P. 2004. Cyanobacterial $H_2$ production - a comparative analysis. *Planta* 218:350–9.

Scranton, M. I. 1983. The role of the cyanobacterium *Oscillatoria* (*Trichodesmium*) *thiebautii* in the marine hydrogen cycle. *Mar. Ecol. Prog. Ser.* 11:79–87.

Scranton, M. I., Novelli, P. C., Michaels, A., Horrigan, S. C. & Carpenter, E. J. 1987. Hydrogen production and nitrogen fixation by *Oscillatoria thiebautii* during *in situ* incubations. *Limnol. Oceanogr.* 32:998–1006.

Seiler, W. & Schmidt, U. 1974. Dissolved non-conservative gases in seawater. *In* Goldberg, E. D. [Ed.] *The Sea*, 5 vol. John Wiley & Sons, New York, pp. 219–43.

Simpson, F. B. & Burris, R. H. 1984. A nitrogen pressure of 50 atmospheres does not prevent evolution of hydrogen by nitrogenase. *Science* 224:1095–7.

Staal, M., Lintel-Hekkert, S., Harren, F. & Stal, L. J. 2001. Nitrogenase activity in cyanobacteria measured by acetylene reduction assay: a comparison between batch incubation and on-line monitoring. *Environ. Microbiol.* 3:343–51.

Stanier, R. Y. & Cohen-Bazire, G. 1977. Phototrophic prokaryotes: the cyanobacteria. *Annu. Rev. Microbiol.* 31:225–74.

Strickland, J. D. H. & Parsons, T. R. 1972. *A Practical Handbook of Seawater Analysis.* Fisheries Research Board of Canada, Ottawa, Ontario, Canada, 310 pp.

Tamagnini, P., Leitao, E., Oliveira, P., Ferreira, D., Pinto, F., Harris, D. J., Heidorn, T. & Lindblad, P. 2007. Cyanobacterial hydrogenases: diversity, regulation and applications. *FEMS Microbiol. Rev.* 31:692–720.

Wilson, S. T., Foster, R. A., Zehr, J. P. & Karl, D. M. 2010a. Hydrogen production by *Trichodesmium erythraeum*, *Cyanothece* sp., and *Crocosphaera watsonii*. *Aquat. Microb. Ecol.* 59:197–206.

Wilson, S. T., Tozzi, S., Foster, R. A., Ilikchyan, I., Kolber, Z. S., Zehr, J. P. & Karl, D. M. 2010b. Hydrogen cycling by the unicellular marine diazotroph *Crocosphaera watsonii* strain WH8501. *Appl. Environ. Microbiol.* 76:6797–803.

## Supplementary Material

The following supplementary material is available for this article:

**Fig. S1.** Replicate analysis of the spectral irradiance experiment (Fig. 4) showing the effect of altering the spectral quality on (a) $C_2H_4$ production, (b) net $H_2$ production, (c) the redox state of the plastoquinone (PQ) pool, and (d) the electron transport rate (ETR), for *Trichodesmium*.

**Fig. S2.** Replicate analysis of the DBMIB manipulation (Fig. 7) showing the effect of incremental additions of the inhibitor DBMIB ($0.5\ \mu mol \cdot L^{-1}$) on (a) $C_2H_4$ production, (b) $H_2$ production, (c) the redox state of the plastoquinone (PQ) pool, and (d) the electron transport rate (ETR), for *Trichodesmium*.

The material is available as part of the online article.

Please note: Wiley-Blackwell is not responsible for the content or functionality of any supplementary materials supplied by the authors. Any queries (other than missing material) should be directed to the corresponding author for the article.